International Journal of Scientific Research in Science and Technology
Print ISSN: 2395-6011 | Online ISSN: 2395-602X (www.ijsrst.com)
doi : https://doi.org/10.32628/IJSRST21869

Analysis of Deformation of Thermoplastics by Using Thermomechanical Process

S. Lingamaiah

Head of the Mechanical Engineering Department and Assistant Professor, S. K. University College of Engineering and technology, Ananthapuramu, Andhra Pradesh, India

Article Info

Publication Issue
Volume 10, Issue 1
January-February-2023

Page Number
86-112

Article History
Accepted: 01 Jan 2023
Published: 09 Jan 2023

ABSTRACT

Nano fluidics has been a major field of research for application in areas like single molecule detection. Most of the research efforts have been concentrated in developing novel nano channel fabrication techniques. Most of these fabrication techniques developed are either expensive or time consuming. NA novel, low-cost fabrication technique to generate sub-micrometer wide channels in thermoplastic chips with potential application in single molecule detection is demonstrated. A custom, mechanical rig was designed, fabricated and optimized to produce a predefined thermo-mechanical deformation in thermo-plastic micro channel chips. Rectangular micro channels with different shapes and sizes were deformed using this rig to optimize the initial microchannel dimensions. Low aspect ratio (height: width) channels with smaller initial dimensions exhibit more potential to reach sub-micrometer widths. However, the nano channel fabrication consistency was adversely affected by manufacturing and assembly tolerances.

Keywords: Micro Channel, Sub-Micrometer, Bulk/Film Micromachining, Surface Micromachining, Mold Micromachining

I. INTRODUCTION

CURRENT NANOCHANNEL FABRICATION TECHNIQUES

Nanofabrication techniques can be broadly classified into two main categories based on the approach taken for fabrication, namely; top-down and bottom-up methods. Top-down methods perform large scale patterning and reducing feature dimensions to nanoscale while bottom-up methods rely on specific arrangement of atoms and molecules to create nanostructures.

Top-down Approach

As the name suggests, in top-down approach nanoscale features are built by machining into a material from top to bottom. This approach can be further classified into three sub-categories:

- Bulk/film micromachining
- Surface micromachining
- Mold micromachining

Bulk/Film Micromachining

In bulk/film micromachining of nanochannels, a channel is etched into a substrate wafer (bulk micromachining) or a thin (few nanometres thick) film deposited on a wafer (film micromachining). This is performed with standard lithography or other advanced lithography methods. The use of lithographic techniques to produce nano-scaled structures is known as nanolithography.

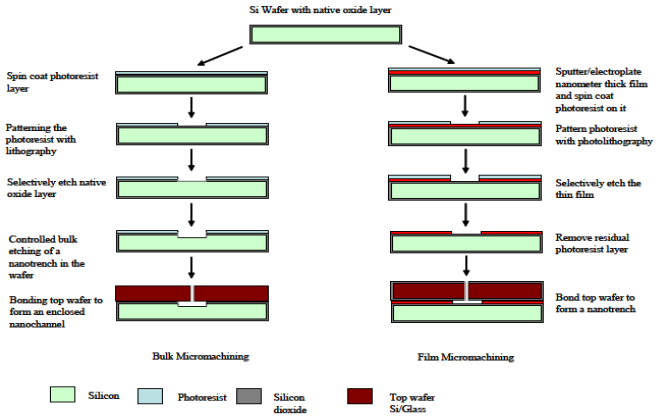

Fabrication process flow in bulk and film micromachining

Standard photolithography techniques have been consistently used to mass-produce channels with widths measuring few micrometers. However, the widths of the channels are limited by the resolution of the photolithographic process used. Typical UV light used in conventional photolithography has a wavelength of around 250 nm. For fabrication of channels with widths less than half of this wavelength, conventional photolithography cannot be used as diffraction will cause blurred features. On the other hand, various technological developments in instruments used in lithography have made it possible to fabricate features in the order of 70 nm with custom experimental setup and about 100 nm in mass production. But these developments have made the process expensive. To reduce the blurring effects due to diffraction and still achieve extremely narrow channel widths, light with extremely small wavelength must be used. X-rays or extreme UV light with smaller wavelengths can be used for this purpose. But conventional lenses are opaque to extreme UV light and cannot focus X-rays.

A combined approach is also demonstrated to develop nano-scaled features by merging the principles of lithography and self-assembly called the hybrid method. Kim et al have demonstrated epitaxial self-assembly of diblock co-polymers on lithographically patterned substrates to produce defect-free, regular and periodic patterns over arbitrarily large areas. In this approach, the nano-scaled structures produced are determined by the size and quality of the lithographically defined topological pattern rather than inherent limitations of self-assembly process.

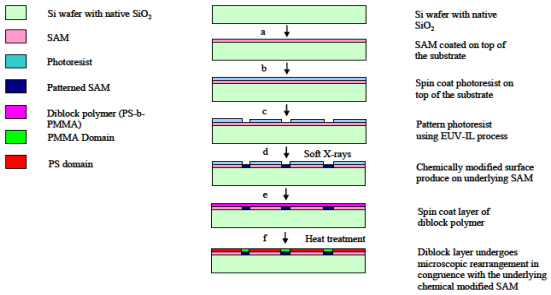

Fabrication process flow for epitaxial self assembly of diblock copolymers

The authors have presented a two step process to develop regular, periodic nanostructures of a diblock polymer, poly(styrene-block-methyl methacrylate) ((PS-PMMA), 104 kg/mol-1, lamellar period approximately 48 nm). In this process lithographically defined pattern in photoresists was used to develop a chemically modified pattern in SAM. This chemically modified monolayer was used to microscopically rearrange the diblock polymer to create these nano-scaled patterns.

A Si wafer with native oxide layer was coated with a self-assembled monolayer (SAM) (Step a). A layer of photoresist was then spin coated on the monolayer (Step b). Photoresist was then pattern with alternating lines and spaces with periods between 45 nm and 55 nm using extreme ultraviolet interferometric

lithography (EUVIL) (Step c) The exposed underlying SAM was then chemically modified by irradiating soft X-rays in the presence of oxygen to produce polar groups on it's surface (Step d).

The photoresist was then removed with repeated solvent treatment. A symmetric, lamella-forming PS-b-PMMA diblock polymer of period 48 nm was spin-coated on this pattern SAM (Step e). Wafer with the epitaxial layers was then annealed above the glass transition temperatures of individual blocks of the co-polymer to diblock copolymer morphologies. The polar groups on the chemically modified SAM provided a surface for preferential wetting by PMMA block and unmodified region exhibit neutral wetting behavior by the block copolymer.

Stoykovich et al have extended this approach to develop non-regular patterns by self assembly of copolymer blends. Instead of just using a diblock copolymer, a ternary blend of diblock copolymers and homopolymers was used to create these nonregular structures.

A ternary PS-b-PMMA/PS/PMMA blend was used for this purpose. The fabrication process essentially remains the same with the SAM being replaced by a poly-styrene brush .

Surface Micromachining

In surface micromachining nano-scaled structures are developed on the surface of a wafer by selective deposition and etching. A bottom layer is first deposited on the surface of a wafer. A nanometer thick sacrificial layer is deposited on the bottom layer and patterned. This sacrificial layer will be etched later to obtain an enclosed structure. A top layer is deposited over the sacrificial layer and patterned to provide access holes for the etchant to reach the underlying sacrificial layer. A nanochannel is thus formed by etching away the underlying sacrificial layer. It can be seen that this approach is similar to film micromachining.

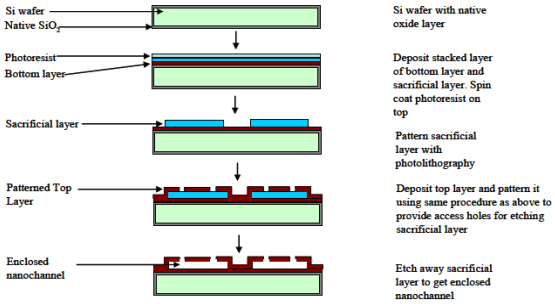

Fabrication process flow in surface micromachining of nanochannels.

The bottom layer is not always required and the sacrificial layer can be directly deposited on the surface of the substrate. But a bottom layer is deposited to form the nanochannel of the same material. If the top and bottom surfaces of the channel are not of the same material, then the fluid flow in the channel can be affected depending upon the nature of the materials that form the channel. Polysilicon is a common sacrificial material but a thermally degradable material can also be used . The main disadvantage of this method is the large amount of time required to etch the underlying sacrificial layer and is therefore not suited for fabricating long channels. Moreover, special access holes are required for the etchant to reach the sacrificial material. Nanostructures can also be damaged during wet etching by the drag forces and also by stiction during drying. Dry etching is a good alternative for wet etching to produce uniform structures without damage.

Mold Micromachining

In mold micromachining, a mold in the inverse shape of the required structure is developed. This mold is then filled with a structural material and later the mold is etched/removed leaving the desired structure behind in the structural material. Poly (dimethylsiloxane) (PDMS) is an example of such structural material. Generation of a PDMS stamp is a quick and easy process and does not require cleanroom environment and is performed by soft lithography. In soft lithography process, the mold is

produced by lithographically developing a pattern (master) in a photoresist or wet/dry etching a pattern in a Si wafer that is used as a template. The pattern is negative of the required pattern in PDMS. PDMS, which is an elastomer is poured on the master template and cured in an oven. After curing, PDMS forms a rubber-like solid which can be easily peeled off the master template leaving behind an imprint from the template. This imprinted PDMS layer can then be covered with another flat PDMS layer to form an enclosed structure like a nanochannel. Soft lithography is a good option for rapid prototyping.

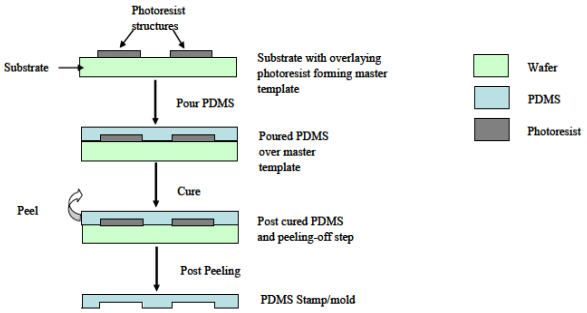

Fabrication process flow in soft lithography

However generation of the master with nanoscaled structures requires use of expensive techniques such as electron-beam lithography. Fabrication of PDMS stamp from master template is cheap and easy process. This PDMS stamp or mold can be further employed for microcontact printing and micromolding in capillaries. In micro-contact printing, the developed PDMS stamp is used as a stencil to transfer its pattern to a surface in contact. In this process, the PDMS stamp is dipped in a solution containing organic molecules and brought into contact with a gold layer on a Si substrate with some applied pressure. These organic molecules are transferred to the gold forming a self-assembled monolayer (SAM) thus reproducing stamp's pattern.

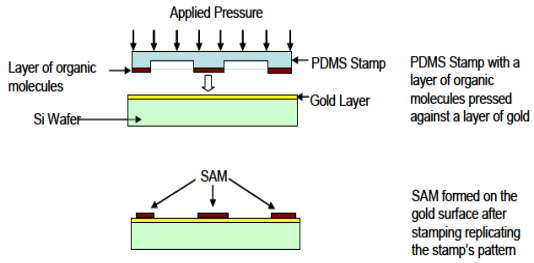

Fabrication process flow in micro-contact printing

On the other hand, in micromolding in capillaries method, the PDMS is placed on hard surface like a glass substrate. A liquid polymer is then passed through the recesses between the stamp and the hard surface by capillary force. The liquid polymer nicely fills all the gaps between the two surfaces. When the liquid polymer solidifies, the PDMS mold can be peeled-off and a molded structure remains behind.

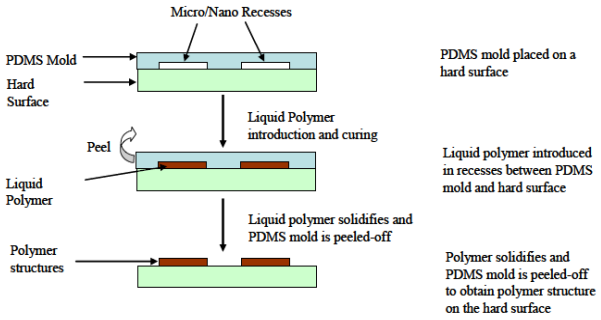

Fabrication process flow in micro-molding process

PDMS is a soft elastomer and therefore prone to deformations and distortions that can lead to errors in the replicated pattern and/or misalignment of the pattern, hence not useful for complex structures. This disadvantage can be overcome by methods such as step-and-flash imprint lithography and nanoimprint lithography (NIL). In NIL, desired nano-scaled structure is embossed into a photoresist, which is then selectively etched to form the desired pattern on the substrate. A thin layer of photoresist is spin-coated on the surface of a substrate. A rigid mold is then pressed against this photoresist layer and whole assembly is heated above the resist's glass transition temperature. This embosses the mold pattern into the resist layer. The residual resist in the thin compressed area can

then be selectively etched away. Thus a pattern in the resist is developed that mimics the master. The master mold can be developed using any of the above-mentioned nano-lithographic techniques. NIL is a fast process well-suited for large-scale production.

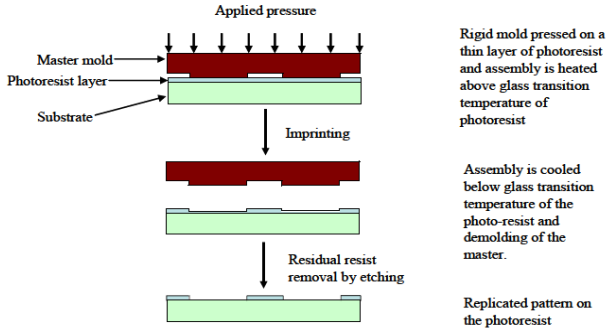

Fabrication process flow in nano-imprint lithography

Features around 20 nm have been reported using NIL. However, the fabrication of master mold is often expensive and any change in the pattern design required a complete new master mold, which is not economical. Moreover, NIL has limitation imprinting micro-scale and nano-scale patterns simultaneously.

Bottom-up Approach

Bottom-up approach relies on systematic assembly of atoms and molecules to form nanostructures through carefully controlled chemical reactions. This is a fairly recent approach and promises to provide cheaper alternative to top-down methods discussed above. Bottom-up approach has been used to fabricate structures like quantum dots and carbon nanotubes. Quantum dots are crystals composed of few hundred molecules, which emit different wavelengths of light when exited with UV-rays, depending on their size. This property has resulted in use of quantum dots as bio-markers. A procedure to create quantum dots consists of a chemical reaction between a metal ion like cadmium and a molecule that can donate a selenium ion. This chemical reaction initiates simultaneous growth of numerous cadmium selenide nanocrystals. In order to prevent these crystals in lumping together to from a macro crystal, the chemical reaction is carried out in presence of organic molecules that act as surfactants, by coating the surface of each cadmium selenide crystal when it grows to a required size. Thus, the chemical reactions initiates growth of cadmium selenide crystals and when they grow a specific size, the organics molecules coat the crystals to form dots. The size of the dots can be controlled by controlling the reaction time. The geometry of the dots can be controlled to some extent by use of different ratios of the organic molecules. Variety of shapes of dots such as spheres, rods and tetrapods can be created. Carbon nanotubes are graphene cylindrical tubes several nanometers in diameter. These nanotubes can be produced by evaporation of solid carbon in an arcdischarge, laser ablation and chemical vapor deposition (CVD) techniques. The structural properties of carbon nanotubes depend on the development process. For example, carbon nanotubes produced by evaporation and laser ablation are in the form of porous membranes and powders that requires further processing, whereas carbon nanotubes can be directly grown on substrates using CVD. Carbon nanotubes with sub-10 nm diameters can be produced. These nanotubes can be used as sacrificial structures to develop enclosed nanochannels.

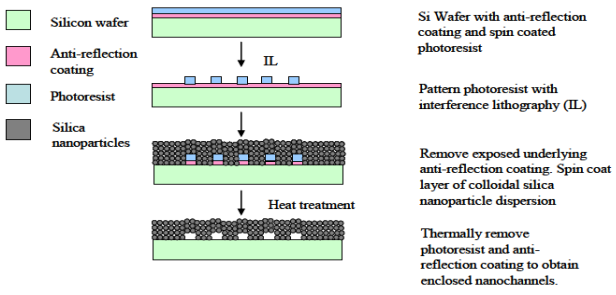

Fabrication of nanochannel by self-assembly of silica nanoparticles

Biologically inspired self-assembly holds promise in bottom-up development of nanostructures. For instance, peptide nanotubes can be self-assembled from cylindrical octapeptides. Self-assembling diblock

polymers as explained above can also be use to fabricate nanostuctures by bottom-up approach.

Bonding

Bonding another substrate to a substrate containing nanotrench is an important step in completing fabrication of an enclosed nanochannel. Methods such as anodic bonding, fusion bonding, and thermal bonding are commonly employed to bond two wafers together. This section will briefly explain anodic and fusion bonding and other polymer bonding techniques. Thermal bonding of polymer nanofluidic chips will also be discussed.

Anodic Bonding

Anodic bonding is a process to bond a glass sheet to silicon wafer. In this process, the glass sheet is brought into contact with the silicon wafer. A high electric voltage is applied across this sandwich. The silicon wafer is kept at a positive potential relative to the glass. When the electric field is applied, positive ions from glass move towards the negative electrode producing a high electric field at the glass-silicon interface. This high electric field produces a large force that pulls the two surfaces together producing a strong bond. The whole process takes place at around 400oC and voltage of the order of 1 kV is applied. Thus nanochannels can be developed in either glass or silicon and a glass cover sheet can be anodically bonded to it to form an enclosed nanochannel.

Fusion Bonding

Fusion bonding is a process to attach two silicon or glass substrates together. In this process, the surfaces of the substrates to be attached are made hydrophilic by creating hydroxyl groups on the attach surfaces.

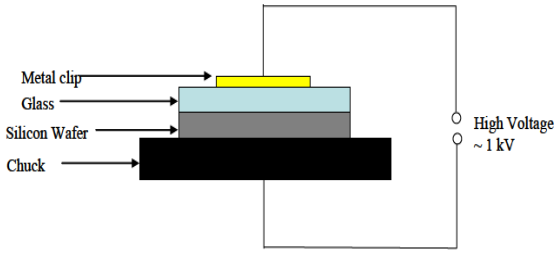

Fusion bonding process

One way of doing this is boiling in nitric acid. Strong hydrogen bonds are formed when the substrates are brought into contact. The bonding process is carried out at a temperature between 300oC to 800oC. High operation temperatures between 800oC to 1100oC can be used to further strengthen the bond.

Apart from anodic and fusion bonding, thermal bonding of polymers is another commonly used technique to bond two polymer substrates. The polymer substrates are heated close to their glass transition temperature and pressed together to form a thermal bond. It is absolutely essential to obtain a good bond in microfluidic chips to prevent any leakage that can affect the performance of the chip. Two main factors affect the bond strength of thermally bonded polymer chips namely, bonding temperature and bonding force. These two factors are inversely proportional to each other. Bonding temperature is more important in terms of getting a good bond without collapsing the imprinted channel network during the bonding process. This is especially critical for imprinted channels with small heights

NANOFLUIDICS FOR SINGLE MOLECULE DETECTION

One of the most promising applications of nanofluidics is in detection ofindividual molecules in fluids. Single molecule detection (SMD) is a methodology to probe a particular individual molecule or sequentially detect an array of individual molecules in a group of molecules. Single molecule detection as apposed to the welldeveloped ensemble methods like liquid chromatography, electrophoresis, massspectrometry provides a more accurate measurement of a parameter under study. In SMD, a study parameter is measured for individual molecule thus providing a distribution of the study parameter for the molecules probed. On the other hand, ensemble methods provide an average value of the study parameter for all the molecules. In analytical chemistry, qualitative as well as quantitative chemical analysis is greatly enhanced by SMD. Moreover, SMD

is beneficial in detection of extremely low concentration of target molecules in a high concentration of normal molecules. Sensitivity of ensemble methods is limited and requires much higher concentration of target molecules for efficient detection. This can be extremely crucial in applications such as detection of early-stage cancer when the concentration of tumor markers is extremely low. Detection of early-stage cancer is crucial to success of tumor treatment surgeries.

II. NANOCHANNEL FABRICATION CONCEPT AND IMPLEMENTATION

This chapter presents the idea behind the nanochannel fabrication technique conceived. A finite element, analytical model used to predict the reduction in the microchannel dimensions under the action of applied lateral, compressive strain is presented. An experimental verification is performed on a PDMS microchannel to assess the feasibility of the nanochannel fabrication approach and verify the concept.

FABRICATION CONCEPT

Various nanochannel fabrication techniques were discussed in chapter one. Lithography was a common method employed in these different techniques. The nanochannel fabrication technique pursued here is a non-lithographic approach to fabricate local nanochannel constrictions along microchannels in thermoplastic microfluidic chips.

This technique relies upon local, thermo-mechanical deformation of a section of microchannel in a thermoplastic chip to form a nanoscaled, in-line constriction. Thermoplastics are polymers that can be formed and shaped when heated and can be reformed over and over again with successive heating. This property has been very attractive to researchers and scientists working in the field of polymer micro and nanofluidics, as complex microchannel networks can be replicated into thermoplastics from a single silicon template, thereby considerably reducing the manufacturing cost and time. Some commonly used thermoplastics are polycarbonate and PMMA. The temperature at which thermoplastics become mechanically pliable is called the glass transition temperature (Tg). Glass transition temperature of any material marks the temperature at which a sudden drop in its elastic modulus is observed. As the temperature of the thermoplastics is increased, their moduli of elasticity decrease making them flexible enough to mechanically deform. This forms the basis of this nanochanne fabrication technique.

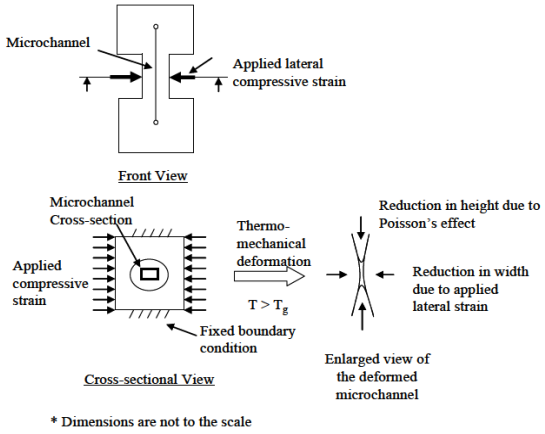

Thermo-mechanical nanochannel fabrication concept

As the lateral, compressive strain is applied on a microchannel, it undergoes deformation in such as way that the width of the channel at its center will undergo maximum reduction, gradually increasing from center to top and bottom of the channel. At the same time, as a result of Poisson's effect, there would be increase in height of the channel. However, if the top and bottom faces of the microchannel chip are mechanically constrained, then the top and bottom sides of the microchannel will undergo a deformation towards the center of the microchannel thereby reducing its height. Thus, under the action of uniaxial, compressive strain, a reduction in two dimensions of the microchannel cross-section can be obtained producing a potential twodimensional nanochannel. Single molecule detection can be performed at the

maximum deformation location, where the microchannel has undergone maximum deformation.

PROOF OF CONCEPT

A plain strain, finite element model was developed using ANSYS® to understand the deformation behavior of a microchannel under the action of applied lateral, compressive strain. Effects of variation in the initial cross-section of the microchannel, i.e. cross-section of the microchannel when no strain is applied, on the final cross section of the deformed microchannel were also studied. Experimental validation of the phenomenon was performed by mechanical deformation of a PDMS microchannel. PDMS is a rubber-like elastomer, which can be deformed easily.

2.2.1 Finite Element Model

A finite element model developed in ANSYS® was used to study the variation in height and width of a microchannel with applied lateral compressive strain and the effect of initial aspect ratio of the un-deformed channel on deformation dynamics. 2D, 8-node, plain strain elements were used for this structural analysis. Since the crosssection of the channel is symmetric about its vertical and horizontal axes, symmetric boundary conditions were applied and only a quadrilateral of the cross-section was used for analysis. Fixed boundary conditions, as explained in preceding sub-chapter, were not applied in the model for deformation of PDMS microchannel, as the primary investigation objective was to understand the reduction in width of the channel along its height with the applied strain and theoretically verify the concept. Increase in the height of the microchannel was also estimated with this model. It was after the investigation of deformation dynamics of PDMS microchannel using this model that the need for fixed boundary conditions was realized and incorporated in the fabrication approach as explained further in this section. The model was modified to incorporate the fixed boundary conditions to study the deformation in thermoplastic microchannel chips. Linear, elastic, isotropic material properties are assumed for simplicity.

The model approach was based on varying the shape of a microchannel inPDMS to understand the reduction in widths of the channel at its center and top/bottom under the applied compressive strain. For a constant microchannel width (5 μm), the height of the microchannel was varied from 1 μm to 10 μm. The applied lateral, compressive strain is increased to a value, where the final minimum channel width reduces to 1 μm and 0.5 μm. This is performed for all 10 cases, i.e. height varying from 1 μm to 10 μm with constant width of 5 μm. The deformation behavior was also studied for microchannel with 10 μm width.

Model Results

Figure 2.2 shows the nomenclature used for the heights and widths of the microchannel at different locations. Variation of the width at the channel center, indicated by 'a' and top/bottom, indicated by 'b', with the applied strain was studied along with the variation in the height of the channel at its center (c). The height of the side-walls was indicated by 'd'.

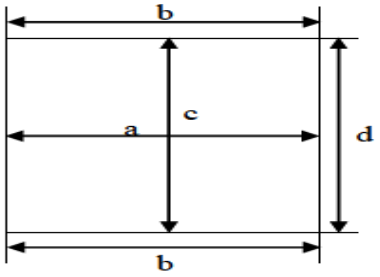

Microchannel cross-section dimensioning nomenclature

a - Width at the center of the channel (micrometers)

b - Width at the top of the channel (micrometers)

c - Height at the center of the channel (micrometers)

d - Height of the side walls of the channel (micrometers)

This dimensioning nomenclature was used in the model results plots for simplification. Note that these are microchannel dimensions and not the dimensions of the cross-section of the plastic chip containing the microchannel. The model results indicated that the deformation in the width (a) at the center of the

channel is higher than the widths (b) at top and bottom of the channel, irrespective of the strain applied and the initial cross-section of the microchannel. The difference between the width at the center and top of the channel increased as the applied strain was increased, indicated by the reduction in ratio of the widths at the center of the channel and at the top of the channel from 1 (no strain applied case, when the side walls of the channel are perfectly vertical) to very close to zero (Fig. 2.3). This means that the channel gets narrower at its center than at top and bottom as the strain is increased. In case of shorter channels, i.e. height (c) less than width (5 μm), for lower applied strain values, the rate of decrease of widths at center and the top/bottom of the channel was almost similar indicated by shallow slope of the plot lines. However, for higher strain values, the width at the center of the channel reduced rapidly than at the top/bottom of the channel. On the other hand, for taller channels the rate of decrease in the width at the center of the channel was higher than at the top/bottom of the channel for all values of applied strain as indicated by the higher slopes of the plot lines for all strain values. For final deformed width of 1 μm at channel center, the ratio of widths at center and top/bottom (a/b) decreased as the initial aspect ratio (height:width) increased. Thus, for taller channels (aspect ratio > 1) when the width at the channel center reduces to submicrometer dimensions, the widths at top and bottom are well above a micrometer. On the other hand, under the action of the applied strain, the height (c) of the channel at its center increased as indicated by the increasing slopes of the lines. Moreover, for taller microchannels, the increase in height of the channel at its center after deformation was higher than for shorter microchannels for the same final deformed width at the channel center (a_final = 1 μm).

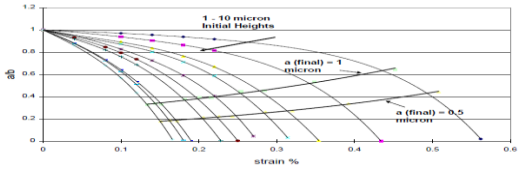

Reduction in widths of the microchannel at center and top/bottom with applied strain

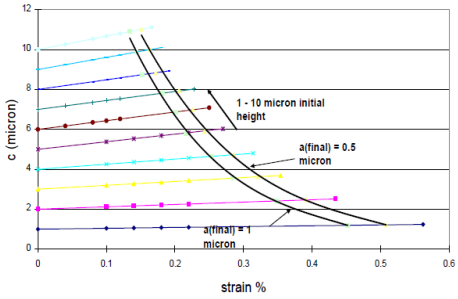

Increase in height of the channel at its center with applied strain

The model results indicated that under the action of lateral compressive strain, the rectangular cross-section of the microchannel undergoes a deformation to an hour-glass shaped outline with only some part of the cross-section in sub-micrometer region. Thus, it was imperative to reduce the difference in widths at the center and top/bottom of the deformed microchannel to get a consistent sub-micrometer channel dimensions. This was achieved by applying fixed boundary conditions on top and bottom faces of the microchannel chip during the thermo-mechanical deformation process. The top and bottom faces of the microchannel chip are the faces of the thermoplastic chip parallel to the microchannel length and perpendicular to the chip thickness. This fixed boundary condition would force the top and bottom horizontal sides of the microchannel cross-section to bend towards the channel center, thereby reducing its height. Thus, during the deformation procedure, the rectangular cross-section of the microchannel will reduce in all directions. As a result, the initial longer curvature of the microchannel sidewalls after deformation is replaced by just a small section of that curvature thereby keeping the width of the deformed microchannel below micrometer along its height.

This finite element model was further modified to incorporate the fixed boundary conditions on the faces of the microchannel chip. Here, a microchannel in PMMA is considered with the actual cross-section of the chip used in the development process. The channel is 10 μm wide and 5 μm high. Lateral, compressive strain is applied to deform the width of the channel at its center to 1 μm and 0.5 μm. It was observed from the model results that due to the fixed boundary conditions, the top and bottom sides of the channel bend towards the center of the channel.

As a result of incorporation of fixed boundary conditions in the model, when the width at the center of the channel reduced to 1 μm from 10 micrometers, the height of the channel at its center reduced to 1.32 μm from 5 micrometers. At the same time, when the width at the channel center reduced to 0.5 μm, height of the channel at its center reduced to 0.76 μm from 5 micrometers. Thus potentially, a one-dimensional nanochannel can be obtained with inclusion of fixed boundary conditions during the thermo-mechanical deformation.

Experimental Validation

The purpose of experimental validation was to quickly verify the trend in deformation of the channel width and height under the action of applied strain. A compressive, lateral strain was applied on a square microchannel (5 μm x 5 μm) in PDMS. The microchannel was prepared in PDMS by soft lithography methods as explained in chapter 1. SU8, a negative photoresist was patterned on a silicon wafer with a native oxide layer to form a master template for soft lithography. PDMS is poured on the template to form a 0.5 mm thick layer. The volume of the PDMS can be adjusted so as to form an approximately 0.5 mm thick layer. The PDMS layer was then peeled-off from the template with imprinted channels and was capped with another flat, 0.5 mm thick PDMS layer to form an enclosed microchannel. The PDMS enclosed microchannel was cut using a 200 μm thick blade in such as way that the width of the PDMS enclosure was approximately 1 mm. Thus, the cross-section of PDMS enclosure was around 1 mm x 1 mm, with microchannel roughly at its center. A compressive, lateral strain was applied with two identical mechanical micrometer linear stages from Newport Corporation†. The cut PDMS microchannel was placed between two flat plastic plates attached firmly to the linear stages. A specific strain can be applied to the microchannel by providing precision displacement using the micrometer linear stages. The deformation in the cross-section is observed under an optical microscope.

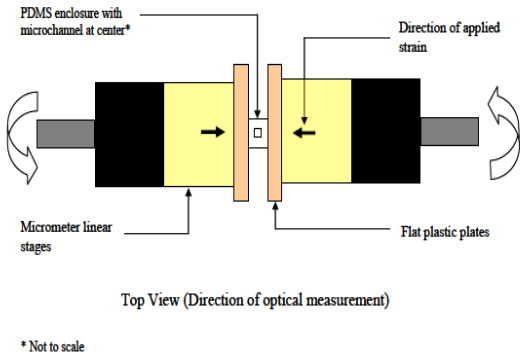

Experimental setup for PDMS microchannel deformation

The experimental data indicated a similar trend in the microchannel width and height variation with the applied strain. The differences in the experimental and model data can be attributed to the model assumptions along with several manual and experimental limitations.

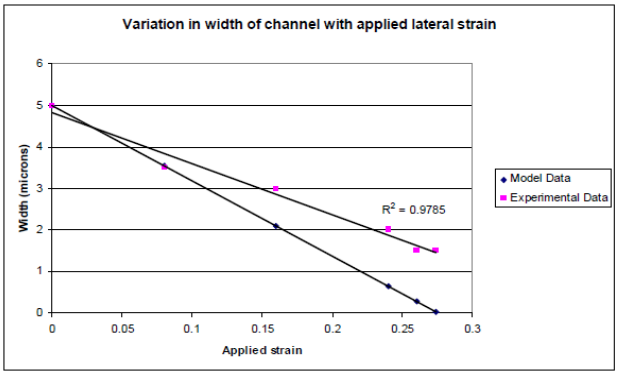

Reduction in width of microchannel in PDMS with applied lateral,

compressive strain

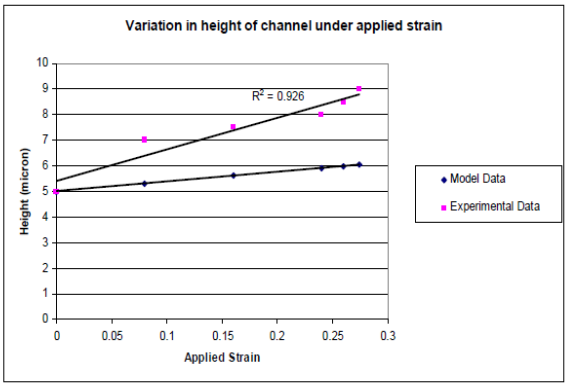

Increase in height of the microchannel in PDMS with applied lateral, compressive strain

A plane strain analysis was assumed for the finite element model developed. The underlying assumption for a plane strain analysis is that the strain in the direction perpendicular to the deformation plane is negligible. Hence in this case, the strain in the direction of the observation (i.e. perpendicular to the PDMS cross-section being observed) should be negligible as compared to the strain in plane of deformation.

However, since the observed cross-section was a free-surface, the strain in the direction perpendicular to the free surface, i.e. perpendicular to the applied strain's plane was considerably high. This contributed to the discrepancy between the plane strain model results and experimental data. There were fabrication limitations in precisely cutting the PDMS enclosure to get the microchannel exactly at its center. Any deviation in the microchannel position from the center of the PDMS cut-out will lead to asymmetry causing unexpected deformation dynamics. The cross-section of the PDMS enclosure formed a bulge in the direction of observation due to the Poisson's effect of the applied lateral, compressive strain. Thus at higher magnification optical detection, the whole microchannel crosssection was not in a single plane of focus, as a result of which a blurred image of the deformed channel was observed. It thus became hard to measure the deformed channel dimensions. This aggravated at higher applied strains. The measurements were further worsened by external noise such as vibration.

THERMO-MECHANICAL DEFORMATION APPROACHES

Various thermo-mechanical deformation approaches to produce a predetermined, lateral compressive strain were evaluated. These approaches were primarily based on the mode of microchannel chip-heating employed and the strain application method. One dimensional heat conduction and convective heating were the two chipheating methods employed. Lateral and vertical strain applications were the two strain application modes considered. Lateral and vertical strains imply the direction of the strain applied with respect to the chip plane. The initial microchannel dimensions used were 100 μm x 50 μm (width x height). Such bigger microchannels were used to first check the feasibility of the approaches under consideration to provide controlled, thermo-mechanical deformation to produce nanochannels.

Approach 1: One dimensional conductive heating and lateral compressive strain application

In this method, the plastic chip was placed on a highly polished, ceramic heating plate. The heating surface of the plate was set to a temperature just above glass transition temperature of the plastic. Polycarbonate chips were used in this case with glass transition between 145oC and 150oC. The surface of the heating plate was set at 160oC. A polished steel plate was placed on top of the plastic chip so as to keep uniform thermal boundary conditions on top and bottom of the chip as the chip heats up. Since steel has high heat capacity, it will reach a temperature close to the heating temperature. A thermocouple was attached to the plastic chip at the steel plate interface. The chip was heated until the thermocouple displayed a constant steady state temperature. The red arrow indicates the direction of heat flow. An aluminum plate attached to a micrometer linear stage was used as probe to produce

lateral strain on the chip. The faces of this aluminum probe were polished so as to provide uniform strain perpendicular to the channel length. However, it was observed that the temperature varied considerably across thickness of the plastic chip. A temperature difference of about 20oC was observed between the heating surface and top of the plastic chip. Thus the modulus of elasticity will vary across the plastic chip, which will affect the deformation dynamics and therefore this approach was not further pursued.

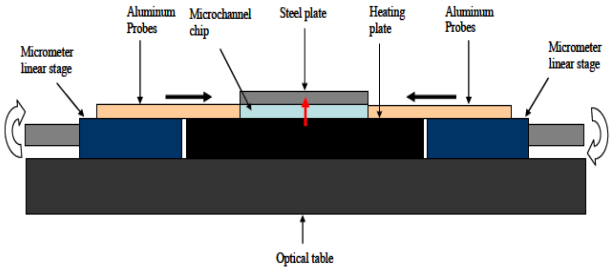

Experimental setup of conductive microchannel chip heating and lateral strain application

Approach 2: Combined conductive and convective chip heating and lateral compressive strain application

It this approach, the plastic chip with the micro-channel at its center was placed on a polished ceramic heating plate set at a temperature just above the glass transition temperature for the plastic. A heating gun was placed vertically above the chip. The heating gun was set to a temperature so that the temperature of the hot air at the chip top surface was close to hot plate temperature. The lateral strain was provided by polished al uminum plates attached to mechanical micrometer linear stages similar to the previous approach. This arrangement was used to ensure similar thermal boundary conditions on top and bottom of the chip. However, it was observed that the plastic chip temperature was considerably less than the heating plate temperature (around 20oC temperature difference was observed). This can be attributed to the thermal resistance between the plastic chip and the heating plate and also the thermal resistance provided by the chip itself. The thermal conductivity of the plastics is very low, which results in higher thermal resistance. The temperature distribution on top of the chip is not uniform as the temperature in a plane from the heating gun tip is not uniform, which resulted in non-uniform heating of the top surface of the chip. Thus, the temperature of the chip remained below the glass transition temperature and the chip could not be deformed using this setup. The heating plate was set 40oC and 60oC above the glass transition temperature of the plastic to increase the temperature of the microchannel chip, however bubbles of trapped hot air from the heating gun were observed in the top part of the chip.

Due to theses problems, this approach was not used for the required thermo-mechanical deformation.

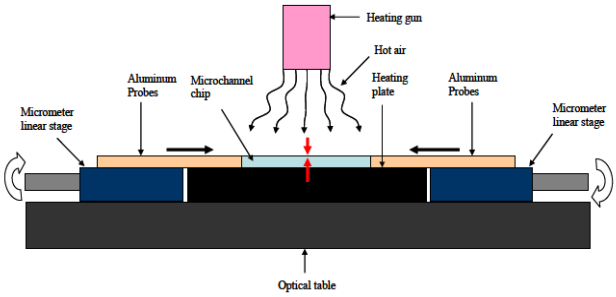

Experimental setup of combined microchannel chip heating and lateral strain application

Approach 3: One-dimensional heat conduction and vertical strain application

The purpose of this approach was to check the application ofPoisson's effect to laterally compress the microchannel to nanoscale by applying verticalstrain. In this approach, the microchannel chip was placed on a polished heating plate.

Two vertical, plate probes placed on either side of microchannel were used to provide the vertical strain. 400 μm thick and 5 mm wide aluminum plate probes attached to a mechanical micrometer actuator were used for this purpose. The distance between the probes was varied from 1 mm to 5 mm in steps of 2 mm. For a 3 mm thick chip, vertical displacements

from 200 μm to 1000 μm in steps of 200 μm were applied with the probes mounted on vertical, linear micrometer stages. It was observed that the channel collapsed before reducing into the submicrometer dimensional regime. Since one dimensional conduction was used, the temperature of the chip at the top of the chip was about 60oC less that the heating plate surface temperature. This can be attributed to the thermal resistance provided by the gap between the plastic chip and the heating surface and thermal resistance along the thickness of the chip. As a result, a much higher temperature was required to be set so as to make sure that the temperature on top surface of the chip is above the glass-transition temperature for the plastic deformation. Thus the modulus of elasticity of the chip increases from the bottom to the top surface. The chip was thus softer at its bottom surface, which was in direct contact with the heating plate and relatively harder at its top surface, where a vertical strain was applied. Thus, as the applied strain increased, the chip being softer at its center, where the microchannel is located, collapsed the channel completely.

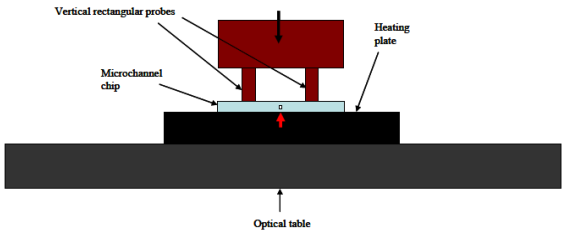

Experimental setup of one-dimensional conductive heating and vertical strain

It was concluded from the above-described approaches that uniform heating of the microchannel chip was crucial to ensure proper deformation dynamics under the action of controlled lateral compressive strain. This will in-turn determine the nature of the nanochannel formed. Heating the chip in a convection oven would provide a more uniform heating of the chip. This lead to the design of a compact, custom, mechanical rig that can ful fill the above requirements.

FINAL IMPLEMENTATION

A custom, mechanical rig was designed, developed and optimized to thermo-mechanically deform the thermoplastic chip in order to obtain local nanochannel constriction in the microchannel. The two main functions of this mechanical rig are: hold the chip vertical with the channel perpendicular to the deformation probes and provide a pre-determined, lateral, compressive strain to the microchannel chip. The rig is compact enough to be placed in a desktop convection oven.

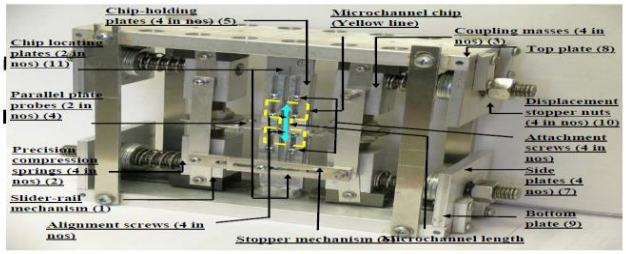

Custom mechanical rig for thermo-mechanical deformation of the microchannel chip

The mechanical rig is an all-aluminum assembly with stainless-steel, precision, compression springs to provide the required strain in the thermoplastic microchannel chip. The main parts of the rig are slider-rail mechanism (1), precision compression springs (2), coupling masses (3), parallel plate probes (4), chip holding plates (5), stopper mechanism (6), side plates (7), top and bottom plates (8,9), displacement stopper nuts (10) and the chip locating plates (11). The microchannel chip is held vertically between the two chip-locating plates using four chip holding plates with alignment and attachment screws. The chip locating plates are two, 1/8th inch (3.175 mm) thick aluminum plates precision welded to the top and bottom plates, so that they are perpendicular to the top and bottom plates. These chip holding plates have slots, which provide openings for alignment and attachment screws to hold the chip between the chip-locating plates. The slots also provide degree of freedom along its length, which is essential for chip mounting process. The alignment screws ensure that the microchannel in the plastic chip is perpendicular to the plate probes. A diameter

clearance of 0.5 mm is provided between the alignment holes drilled in the microchannel chip and the alignment screws to compensate for manufacturing and alignment tolerances. The chip holding plates are screwed to the chip locating plates with the microchannel chip sandwiched between the chip-holding plates. The alignment screws along with the chip holding plates prevent any motion of the chip relative to the plate probes during the indentation process. The chip-holding plates also ensure that the plate probes move in one plane during the deformation process, thereby eliminating/reducing any offset in co-linearity of the plates. The coupling masses attached to the slider mechanism transfer the expansion of the compression springs to the aluminum plate probes through horizontal and vertical threaded rods that results in lateral compressive strain on the vertically held chip. The slider is made out of ceramic-lined aluminum and slides over an aluminum rail. Thermal grease is applied between the slider and rail to reduce friction effects due to thermal expansion while operating at deformation temperature (~120oC). Symmetric arrangement of the compression springs eliminates bending in the probes. Precision compression springs pass over horizontal, 0.5 inch threaded rods (1/2"-13†) connected to the coupling mass. These threaded rods pass through clearance holes in the sides plates, which are attached firmly to the base and top plates. A similar assembly is made on the top plate and the coupling masses on these assemblies are connected together through vertical, 0.5 inch threaded rods (1/2"-13). The parallel plate probes are held firmly between two lock nuts on these threaded rods. This arrangement provides position adjustment of the probes along the threaded rods for their in-plane alignment. The top and bottom plates are connected together with four, 1/8th inch aluminum plates. Nuts placed on the horizontal rods are used as displacement stopping devices. Thus, these nuts can be placed at a distance from the side plates that will decide the extent of compressed spring expansion and thereby the compressive strain applied to the chip. The distance between the stopper nuts and the side plates can be decided by the number of revolution of the nuts over the threaded rod (1 revolution = 1.96 mm or 2 mm approximately). The stopper mechanism consists of a tightening screw and nut assembly passing through two slotted aluminum plates. The friction between the tightened screws and the aluminum plates prevents the compressed springs from expanding until the screw is loosened. The stopper mechanism ensures that no indentation is produced on the chip until the rig and the chip reach a steady-state thermal condition. Once the assembly reaches preset temperature in the convection oven, the screw can be manually loosened to initiate the expansion in the compressive springs thereby providing gradual, lateral, compressive strain on the microchannel chip.

III.NANOCHANNEL FABRICATION PROCESS

The nanochannel fabrication process developed can be divided into three major steps: master template generation, microchannel chip manufacturing and thermomechanical deformation of the microchannel to nanoscale. A <100> silicon wafer was used to generate the master template with standard photolithography and deep reactive ion etching (DRIE). A PMMA chip containing the microchannel was generated from Si master template, developed in step 1, with hot embossing and thermal bonding techniques. Final chip with nanochannel constriction was developed by directed mechanical deformation of the heated microchannel polymer chip, using the custom mechanical deformation rig. The nanochannel chip can further be post-processed (milling and mechanical polishing) for application in optical detection of single molecules.

MASTER TEMPLATE GENERATION

Master template generation consists of two steps: photolithography and deep reactive ion etching (DRIE). In the first step, a photoresist pattern was

developed on the Si wafer surface, which was further used as a mask for DRIE. DRIE dry etching further transfers the topographical photoresist pattern to the Si wafer, creating rectangular structure on the wafers surface. The structures on etched Si wafers were further hot embossed on PMMA wafers. The pattern consists of microchannels, 25 mm long and widths varying from 5 micrometers to 25 micrometers.

Photolithography

A 4 inch, virgin <100> Si wafer was rinsed in solvents (Acetone, Methanol and IPA) to clean its surface and baked over-night at 120oC. Baking ensures proper removal of moisture from the substrate's surface, which results in better adhesion for the photoresist on the wafer surface.

The silicon wafer was vacuum held on a wafer-chuck in SCS G3P-8†† spincoater. Few drops of Hexamethyldisilazane (HMDS) were put on the wafer surface and allowed to stand for 3 minutes. HMDS is then spin-coated at 4000 rpm for 30 seconds to form a thin layer on the wafer surface. HMDS was used to enhance the adhesion between the wafer surface and the coated photoresist. The positive photoresist, AZ® 9245 was spin coated on the surface of the wafer to form a 4.5 µm thick layer. The spinning was done at 3000 rpm for 30 seconds. The resist coated wafer was pre-baked at 90oC for 2 minutes to remove any excess moisture. The pre-baked wafer was exposed to UV light (wavelength ~ 250 nm) for 150 seconds at a dose of 6.5 mW using Karl Suss MA6 Mask Aligner‡‡. A soda-lime, chrome mask is used in this step. To achieve fine channel widths to the order of 5 µm, film mask cannot be used. The exposed wafer was post-baked at 90oC for 2 minutes to enhance adhesion between the unexposed resist and the wafer. The exposed wafer was developed in AZ® 400K‡ developer solution for about 3 minutes. A combination of immersion and spray development techniques was used to make sure that narrow structures do not delaminate from the wafer surface. It was observed that only immersion development delaminated 5 micrometer wide structures from the wafer surface. The Si wafer was dry etched using deep reactive ion etching machine. The wafer was exposed to give required etch depth. One cycle of DRIE was composed of 10 seconds of etching and 6.5 seconds of passivation step. 14 cycles gave an etch depth of 5 µm and 9 cycles gave an etch depth of 3 µm. DRIE gives vertical side-walls, which are crucial for the nanochannel development process. Before etching, the wafer with photoresist pattern was treated with oxygen plasma for 8 seconds.

After DRIE, the photoresist was stripped-off from the wafer surface by immersing in Nanostrip®† for 2 hours at 60oC. The Si wafer was then used as a master template for hot-embossing its pattern on thermoplastic (PMMA) wafers.

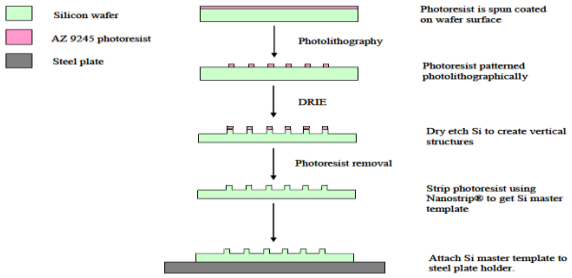

Fabrication process flow for lithography

Template preparation

The developed Si wafer was attached to a smooth steel plate using Pyralux®† LF adhesive sheet. This attached wafer was further used in Carver Hot Press for hot embossing PMMA wafers.

The Si wafer was placed on a 1/8th inch (3 mm) polished steel plate ((6 inch x 6 inch) or (153 mm x 153 mm)) with the Pyralux® sheet in between. A 0.5 inch (6.35 mm) thick glass plate ((5 inch x 5 inch) or (127 mm x 127mm)) was placed on top of the Si wafer with a Teflon sheet in-between. The Teflon sheet prevents any minute relative lateral motion of the platen of the hot press with respect to the sandwiched layers from transferring to the silicon template while opening the platens, which can shear-off the structures on the Si template.

The sandwich was placed between two hot platens of the Carver Auto Four/15 Hot Press. The platens were set at 170oC. A pressure of 238 psi (1641 kPa) was

applied on the sandwiched assembly for 3 hours. The Si template sticks to the bottom steel plate and can be further used for hot embossing polymer wafers.

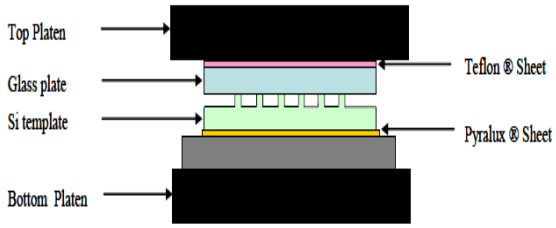

Assembly for template preparation.

MICROCHANNEL CHIP MANUFACTURING

This step consists of hot embossing the Si template pattern into a PMMA wafer followed by thermal bonding of a PMMA cover slip with inlet and waste reservoirs to the embossed wafer. This is done in a Carver Auto Four/15 Hot Press.

Hot Embossing

The master Si template was mounted on lower platen of the hot press with the help of a template holder. Make sure that the template is firmly held on the platen so that there is no relative motion of the template with respect to the platens, which can damage the template or imprinted pattern. Tightening screws were used to ensure this. A 4 inch, 1.5 mm thick PMMA wafer was placed on the master Si template. The PMMA wafer was degassed in a heated (80oC) vacuum oven overnight. A glass plate (same dimensions as explained above) was kept on the PMMA wafer with a Teflon sheet in-between them, forming a sandwich layer of Si template, PMMA wafer, Teflon sheet and glass, bottom to up respectively. A Teflon sheet separates the glass plate from the top platen. The platens' temperature was set to 145oC. A pressure of 100 psi (690 kPa) was applied to the arranged PMMA - Si template sandwich for 20 minutes. The dwell time ensures complete heat transfer to the PMMA wafer for proper reflow of the material resulting in proper pattern transfer. The assembly was cooled down to a temperature just above the glass transition temperature for PMMA (105oC) and the applied pressure was removed. (If the pressure is removed at a temperature lower that the glass transition temperature of PMMA, then silicon from the template sticks to the PMMA wafer and gets removed from the template surface during demolding of the PMMA wafer). The assembly was then further cooled to 85oC. The imprinted PMMA wafer was demolded with the pattern transferred from the template. The imprinted side of the imprinted wafer was covered with a blue tack tape† to prevent any dust particles from clogging the channel.

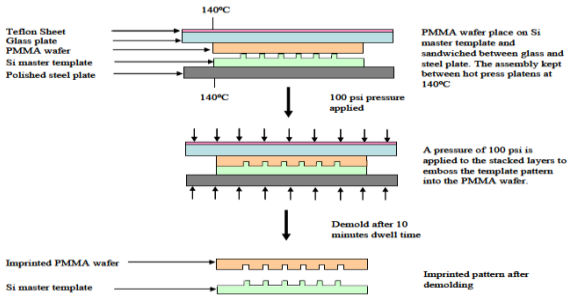

Fabrication process flow for hot embossing PMMA wafer

Thermal Bonding

Input and waste reservoir holes were drilled in the PMMA cover plate (Acover plate is a 4 inch in diameter, 1.5 mm thick PMMA wafer that is thermally bonded to the imprinted wafer to form an enclosed microchannel). The holes were drilled at locations such that they aligned with the imprinted channels on the embossed PMMA wafer, when the two wafers are put together. The drilled holes were deburred to prevent] any clogging of the channel near the reservoirs after bonding.

The PMMA cover plate was placed on the imprinted PMMA wafer so that the drilled holes aligned with the corresponding imprinted channels. These two wafers were then sandwiched between two glass plates. The whole assembly was placed between the platens of the Carver hot press, which were set at 95Oc.

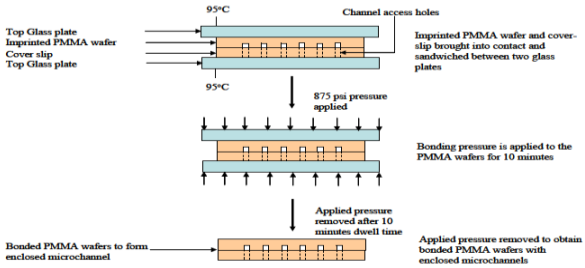

Fabrication process flow for thermally bonded PMMA wafers

A pressure of 1200 psi (8273.7 kPa) was gradually applied to the sandwiched PMMA wafers with increasing platen temperature. The pressure was maintained on the assembly for 15 minutes to ensure complete heat transfer to the sandwiched PMMA wafers for proper bonding.

The applied pressure was removed and the bonded PMMA wafers were allowed to gradually cool down. If the wafers are cooled down rapidly, then they can delaminate due to thermal shock. The input and waste reservoirs on the bonded wafers were covered with blue tack tape to prevent particulates from entering the channel. With this bonding process, very small reduction in imprinted channel height was observer (< 0.5 μm). Individual custom-shaped PMMA microchannel chip were cut out of these bonded PMMA wafers.

Wafers were also bonded using UV-ozone treatment. The surfaces of the imprinted wafer and the cover plate were UV-ozone treated for 10 minutes each. The wafers were then bonded at 90oC with bonding force of 11000 lbs (48.93 kN). However, during the thermo-mechanical deformation, local flower shaped spots were observed, which can be local delamination or modification of the bond surface due to some unknown chemical reaction initiated by the UV-ozone treatment. Considerable delamination was also observed along the microchannel after thermo-mechanical deformation. This was consistently observed for all UV-ozone treated chips.

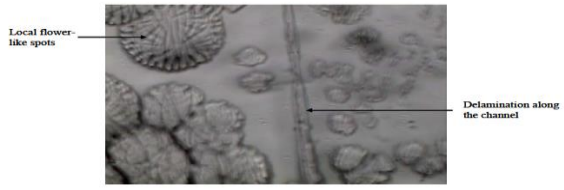

Flower-like spots in a UV-ozone treated chip after heat treatment

THERMO-MECHANICAL DEFORMATION

During the thermo-mechanical deformation process, a section of the microchannel in the thermoplastic chip was constricted to nano-scale with the customdesigned, mechanical deformation rig. This process consists of two important steps, namely: individual chip cutting into a custom shape to fit in the rig and the chip mounting in the rig.

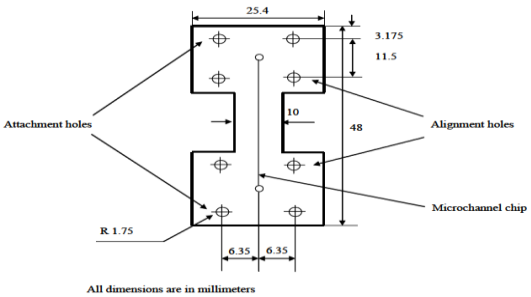

Custom-shaped plastic microchannel chip before thermo-mechanical deformation

Alignment holes and attachment holes (3.5 mm in diameter) were drilled symmetrically adjacent to the microchannel in the thermally bonded PMMA wafers. The bonded wafers were then cut into rectangular shapes (25.4 mm x 48 mm). Two slots were milled in these individual, rectangular chips so that the microchannel was located at the middle of a 10 mm section. Milling ensured flat machined surface, which was critical for uniform compressive strain on the channel. At no applied strain condition, the parallel plate probes slide into these slots and touch the chip at the milled surfaces of the chip at equal distance from the microchannel.

Microchannel Chip Mounting Procedure

The custom-shaped microchannel chip was mounted between two aluminum, chip locating plates welded at the center of top and bottom plates of the

mechanical rig with the help of chip-holding plates. These aluminum plates were precision welded so that they are perpendicular to the top and bottom plate planes. Custom-shaped, thin, aluminum plates were sandwiched between the chip-holding plates and the microchannel chip to provide fixed boundary conditions on both faces of the chip. These thin aluminum plates are similar in shape to the microchannel chip, but with a narrower section at the center.

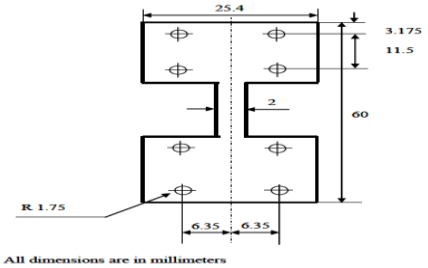

Thin aluminum plate to provide fixed boundary conditions on chip faces

Narrower section was required to ensure that the plate probes can produce indentation and were not stopped by these aluminum plates. Thus the PMMA microchannel chip was vertically held at the center of the rig between the chip locating plates, with a holding assembly configuration of chip holding plates on the outside, followed by the thin aluminum plates for fixed boundary condition on either side of the microchannel chip and the chip at the innermost position in the sandwich. Following was the chip mounting procedure developed. First ensure that the plate probes are away from the location where the microchannel chip is going to be mounted (i.e. between the chip locating plates). The displacement stopping nuts hold the compression springs from expanding.

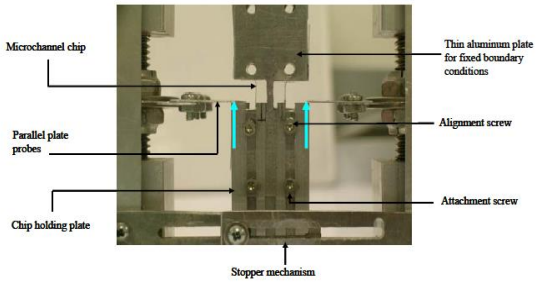

Assembly of lower chip holding plates, aluminum plates and microchannel chip

An sandwich assembly consisting of the chip holding plates (2 in number), thin aluminum plates (2 in number) and the microchannel chip was aligned with the vertical chip locating plate welded to the bottom plate with the help of two, 1 inch long 4-40† screws passing through the attachment holes and two similar screws passing through the alignment holes. The chip holding plates were slid towards the parallel plate probes so that they just touch the probes. The screws through the attachment holes were tightened to firmly hold the assembly. This assembly will be below the parallel plate probes. A similar assembly was performed on top of the plate probes. The top and bottom chip holding plates were thus separated by a small gap in which the plate probes slid during the expansion of the compressed springs, thus providing the necessary compressive strain in one plane.

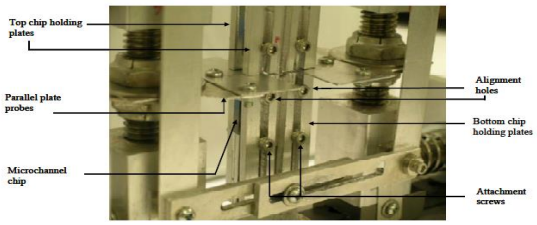

Complete assembly of vertically held chip with of chip-holding plates

This assembly prevented/reduced any offset in deformation planes of the probes along the microchannel length, which would have caused the channel to undergo displacement/bending during deformation, thereby reducing the efficiency of the rig. The displacement stopping nuts on each side of the rig were rotated in anti-clockwise direction so that the compressed springs started expanding, which resulted in motion of the plate probes in the gap between the chip holding plates towards the vertically held chip. When the plate probes touched the sides of the chip, the screw in the stopper mechanism was tightened. At this point, the load on displacement stopping screws will reduce considerably, as the load due to the compressed

springs will be shared by the plastic microchannel chip and the stopper mechanism.

Each of the displacement stopping nuts was further rotated in anticlockwise direction to set a displacement that needs to be provided to the plate probes during the thermo-mechanical deformation process. One rotation of the nut on the horizontal ½"-13 threaded rod will result in 1.96 mm ≈ 2mm.

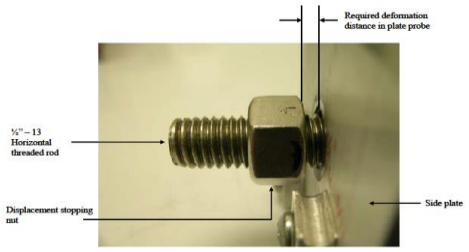

Positioned displacement stopper nut for specific indentation

Thus, the displacement was set depending upon the required strain. The microchannel lies at the center of a 10 mm neck in the custom-shaped plastic chip. Thus, if each of the displacement stopping nuts is placed 2 mm from the side plates, then the displacement in each plate probe will be 2 mm. As a result, the total displacement towards the microchannel will be 4 mm (2 mm in each of the plate probes), giving a compressive strain of 40 %.

After the displacement stopping nuts were set at a required position, the mechanical rig was placed in a convection oven preset at 120oC. A drop in temperature of the oven was observed at this point. When the temperature in the oven again reached a steady state value of 120oC, the screw in the stopper mechanism was unscrewed to loosen the stopper mechanism (approximately 110 minutes for the developed mechanical rig). The compression springs, which were held fixed due to the stopper mechanism underwent expansion, thereby providing displacement to the parallel plate probes. The expansion in the springs stopped when the displacement stopping nuts touched the side plates, thus stopping the displacement in the plate probes and only a pre-determined indentation was produced in the plastic chip.

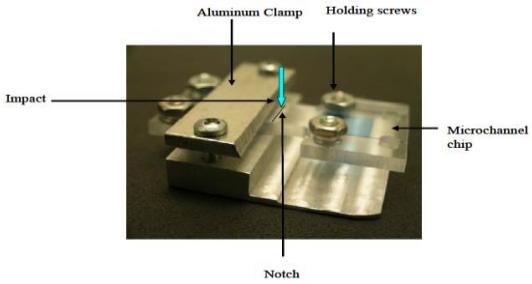

Assembly for cryogenic microchannel chip cross-sectioning

IV. EXPERIMENTAL RESULTS AND DISCUSSION

Microchannels in thermally bonded PMMA chips were thermomechanically deformed at 120oC in a convection oven to constrict the microchannel to nanoscale. Microchannels with different aspect ratios and sizes were deformed at strains so as to reduce the microchannel width to submicrometer dimensions. Three initial microchannel cross-sectional sizes were used here, namely: 10 μm (width) x 15 μm (height) [case 1]; 10 μm (width) x 5 μm (height) [case 2]; 5 μm (width) x 3 μm (height) [case 3]. The thermo-mechanical deformation was performed with and without fixed boundary conditions on the faces of the PMMA microchannel chip for case 1 and with fixed boundary conditions for cases 2 and 3.

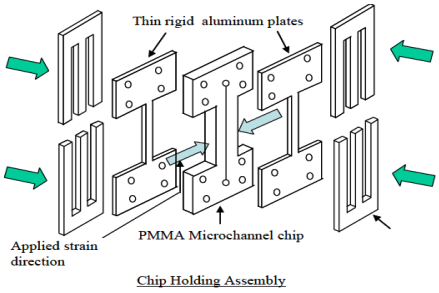

Thin aluminum plates for fixed boundary conditions on the chip faces during thermo-mechanical deformation

Thermo-mechanical deformation with fixed boundary condition implies deformation of the heated microchannel chip in the mechanical rig with the thin aluminum plates covering the faces of the chip, which are perpendicular to the strain application direction Thus the material in the vicinity of the channel along its length is restricted from bulging out,

perpendicular to the chip's face, after deformation. The absence of these aluminum plates during deformation leads to deformation without fixed boundary conditions. The material thus forms a bulge along the length of the channel at the deformation region.

CASE 1: THERMO-MECHANICAL DEFORMATION OF 10 MM (WIDTH) X 15 MM (HEIGHT) MICROCHANNEL

This high aspect ratio† (aspect ratio = 1.5) microchannel was deformed in such a way that the width of the microchannel reduced to sub-micrometer dimension. When the fixed boundary conditions were not applied on the faces of the microchannel chip during the thermo-mechanical deformation, it was observed that the width at the center of the microchannel decreased to sub-micrometer regime (966 nm) for a lateral, compressive strain of 30 %. Moreover, the reduction in width of the channel at its center was highest, thus giving an hour-glass shaped cross-sectional profile, as predicted by the finite element model for high aspect ratio microchannels. Thus, the custom mechanical rig developed was capable of producing the desired effect of thermomechanical constriction of the microchannel to nanoscale dimensions. However, the widths at top and bottom of the microchannel remained above 1μm, thereby creating trans-micrometer sized holes. This will adversely affect the detection efficiency in applications such as single molecule detection. For example, in case of single molecule detection using this channel profile, not all the molecules passing through the nanochannel constriction will be detected by the sub-micrometer wide confocal microscope laser spot, thereby reducing the detection efficiency.

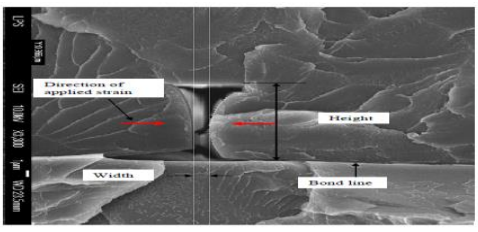

SEM image of a thermo-mechanically deformed high aspect ratio channel.

It was also observed that the top side (side away from the bond line) of the microchannel bent slightly towards the center of the channel and the bottom side away from the center of the channel, in contradiction with the model. This phenomenon was consistently observed in all the chips deformed with this setup. One of the contributing reasons could be the relative motion of the bulk material, perpendicular to the direction of applied strain during the thermo-mechanical deformation process due to bending in the softened microchannel chip. A curvature in the bond line indicated the relative motion of bulk material cause due to bending in the chip along a preferential direction (perpendicular to face of the chip) during thermo-mechanical deformation. To make use of variable width along the height of the deformed microchannel, this high aspect ratio microchannel was subjected to higher lateral, compressive strains with an intention to close the microchannel at the center and create two, one-dimensional, triangularnanochannels, one at the top† and other at the bottom††. The microchannel chip was deformed at 60%, 70% and 80% lateral, compressive strains. It was observed that a submicrometer (height = 896 nm) triangular channel was obtained at the top for 70% strain. At 60% applied strain, the channel at top had a height of 1.5 micrometers. However, a trans-micrometer, rhombus shaped hole was also observed at the bond interface of the chip. Thus, the detection efficiency of such a cross-sectional profile will be less as most of the molecules to be detected will pass through the trans-micrometer hole, which will not be detected by the detection laser.

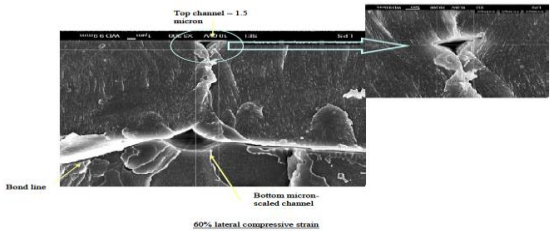

SEM image of thermo-mechanically deformed high aspect ratio channel at 60% strain

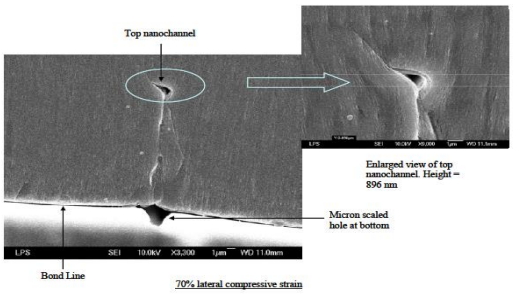

SEM image of thermo-mechanically deformed high aspect ratio channel at 70% strain

Moreover, the production of this one-dimensional nanochannel was not consistent and for other chips deformed at 70% strain, the top triangular channel was completely closed. The variability in motion of the bulk material can be considered as a major reason for the inconsistency of the one-dimensional nanochannel production. The motion of the bulk material depends upon the it's viscosity, which in turn depends on the deformation temperature and the chip's alignment with respect to the deformation probes. At 80% strain, the channel at top completely collapsed. It was thus hard to control the dimensions of the channel at the top, once it reaches submicrometer dimensions. The rig was designed in such a way that the compressive strain can only be applied in steps of 10%. Below this value, precise indentation is not possible.

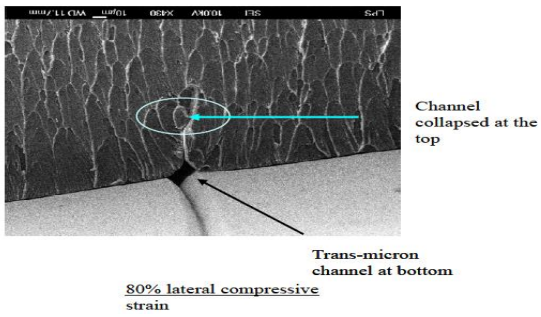

SEM image of thermo-mechanically deformed high aspect ratio channel at 80% strain

In order to restrict the bending at the bottom of the channel and obtain two submicrometer triangular channels, fixed boundary conditions were applied to the faces of the microchannel chip during the thermo-mechanical deformation. It was observed that the bending in the bottom side of the channel away from the channel center that was observed in absence of the boundary conditions, was restricted. But at the same time, the top horizontal side of the channel bent more inwards towards the channel center, thereby closing the channel at the top. A trans-micrometer, trapezoidal channel was developed. Channel with such a cross-section cannot be efficiently used for single molecule detection as the nanochannel volume does not match the laser detection volume.

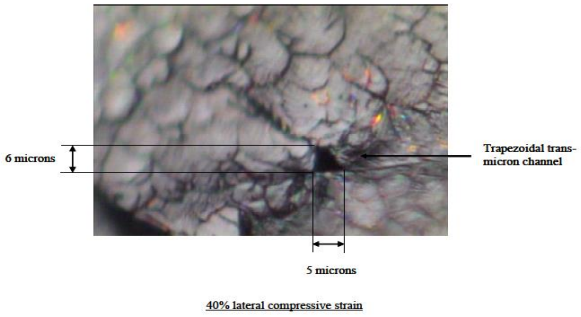

Trapezoidal cross-section of thermo-mechanically deformed high aspect
ratio channel with fixed boundary conditions

Similar results were obtained for 50% applied strain. One of the reasons for the variable deformation characteristics in top and bottom side of the microchannel can be stress concentration near the imprinted channel and at the bond interface. The top side of the microchannel, which is the horizontal side of the imprinted channel, suddenly collapsed under the action of the applied strain. In case of the bottom side, which was provided by the cover-slip after thermal bonding, there could have been a stress accumulation at the bond interface on either side of the bottom side of the microchannel. On the other hand, there would be no stress on the bottom side. This stress distribution across the channel cross-section may be the contributing factor for this irregular deformation nature. Moreover, for a higher aspect ratio channel, there was a considerable decrease in dimensions of the channel for small changes in the applied strain. Thus, smaller irregularities in applied strain, in terms of uniformity

of the strain on either side of the channel, misalignment of the plate probes with respect to the microchannel would have adversely affected the deformation dynamics of the microchannel. A combined effect of the above two causes may have lead to irregular deformation of the microchannel.

CASE 2: THERMO-MECHANICAL DEFORMATION OF 10 MM (WIDTH) X 5MM (HEIGHT) MICROCHANNEL.

A microchannel with cross-sectional dimensions, 10 μm (width) x 5 μm (height) was subjected to lateral, compressive strains varying from 40% to 70%, in steps of 10% with fixed boundary conditions on the chip faces. The deformation temperature is 120oC.

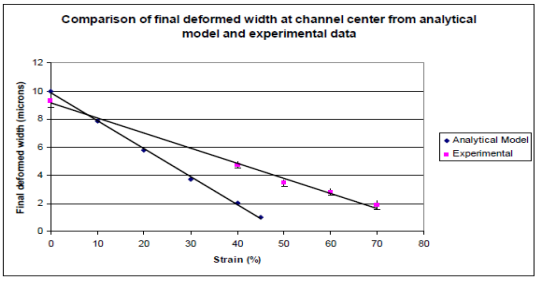

Comparison of experimental and theoretical final deformed microchannel widths

It was observed that the microchannel reduced in all directions, which corroborates the proposed theory in chapter 2. The width reduced to an average value of 1.85 μm from 10 micrometer initial width at a strain of about 70%. On the other hand, the height of the channel reduced to around 0.8 μm from 5 micrometers. When the experimental results were compared with the model results, it was observed that the actual strain required for the channel to reduce to nanoscale or near sub-micrometer dimensions is much larger than theoretical strain (>70% actual strain as compared to 42% in case of model). This discrepancy between the actual and theoretical values can be attributed to the viscous flow of the material during thermo-mechanical deformation. The model assumes an elastic behavior for the deformation process at low applied strains. However, during the thermo-mechanical deformation process, there is viscous flow of the material indicating viscoplastic behaviour at higher strains. The fixed boundary conditions on the faces of the chip prevented any bulk material motion perpendicular to the faces of the chip in the region close to the microchannel during this viscous flow. This offered resistance to the bulk flow of the material towards the microchannel. As a result, the viscous material takes the least flow resistance path and forms bulges on either side of the fixed boundary condition plates.

This reduced bulk material flow of the material towards the channel reduced the efficiency of the rig (i.e. higher strains required to reach sub-micrometer width). Thus a larger strain was required to reduce the microchannel width to near micrometer dimension.

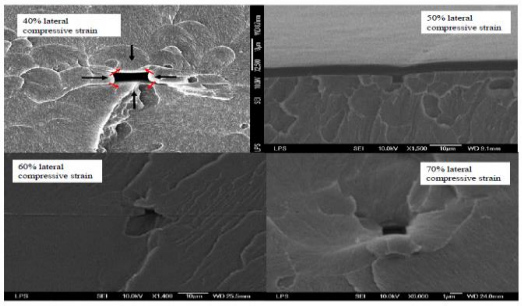

SEM image of thermo-mechanically deformed channel at different compressive strains

Isotropic material properties were assumed in the model. The material properties might not be isotropic depending upon its composition. This could have also affected the deformation dynamics of the microchannel.

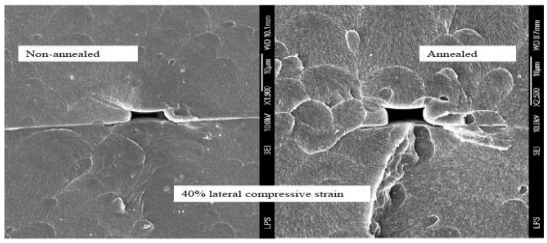

Comparison of thermo-mechanically deformed cross-section for annealed and non-annealed chips

It was also observed that annealing a thermally bonded chip with an embossed channel improved the deformation performance. Annealed and non annealed chips were deformed at same strains, 40% and 50%. The annealed chips showed a greater

reduction in width of the channel as compared to non-annealed chips.

CASE 3: THERMO-MECHANICAL DEFORMATION OF 5 MM (WIDTH) X 3MM (HEIGHT) MICROCHANNEL

To allow the channel width reach sub-micrometer dimensions at lower strains, a microchannel in the PMMA chip with cross-sectional dimensions of 5 micrometers (width) and 3 micrometers (height) was thermo-mechanically deformed at 120oC. Reduction in all the dimensions of the channel was observed as in the previous case. A minimum average width of 1.758 μm was observed for an applied strain of 50 %. The corresponding average height for 50% strain is 1.43 μm.

Similar to case 2, a larger strain is required for the microchannel width to reduce to close to 1 μm when compared to theoretical strain predicted by the model. When the microchannel with these initial dimensions was subject to 60 % compressive strain, the width at the center of the channel reduced below one micrometer (625 nm).

When microchannel with these initial cross-sectional dimensions was further deformed at 70% strain, the deformed channel was observed to be collapsed. This was consistently observed for all the chips deformed at 70% strain. The fabrication method is thus limited in its ability to precisely control the width of the deformed channel within 1micrometer range. This can be attributed to the limited least count of strain application. Lateral compressive strain in steps of 10 % can be applied using the mechanical rig developed. If precise control (< 10% resolution) in strain application is achieved in the
mechanical rig, then the final width of the deformed microchannel can be controlled efficient below 1 micrometer. Moreover, error in manufacturing individual chips for deformation, like width of the narrow section of the individual chip less than 10 mm, could have lead to larger strain induced into the chip than actual strain applied, which could have resulted in channel collapse.

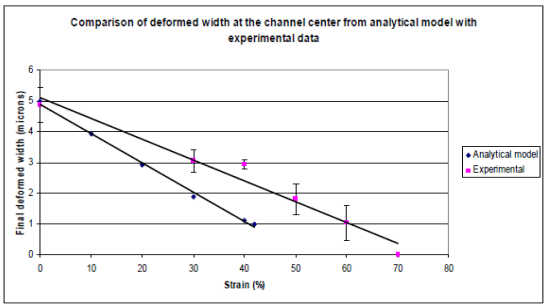

Comparison of theoretical and experimental deformed microchannel widths

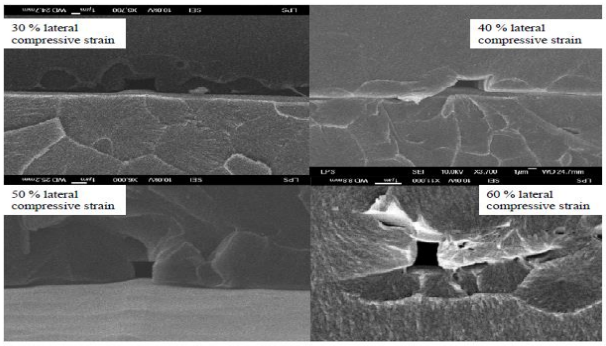

SEM images of thermo-mechanically deformed microchannel at various compressive strains

The possible cause for this difference in required strain as predicted by the model and actual required strain is same as explained above. However, a final width below 1 micrometer was observed at a lower strain (60%) in case 3 as compared to the case 2 (70 %). Moreover, the microchannel width did not reduce below 1 micrometer for case 2. When the reduction in height for the above two cases was compared, it was seen that the reduction in height of the channel in case of the 10 μm (width) x 5 μm (height) channel is more than 5 μm (width) x 3 μm (height) channel. The initial width of the microchannel in case 2 was greater than case 3, which allows the top and bottom sides of the microchannel to bend more at center under the action of applied strain. Thus in case 2, in which the width of the microchannel reduced from 10 μm to around 1 micrometer dimension, a larger bending in top and bottom sides occurred, resulting in smaller height of the deformed microchannel as compared to the case 3.

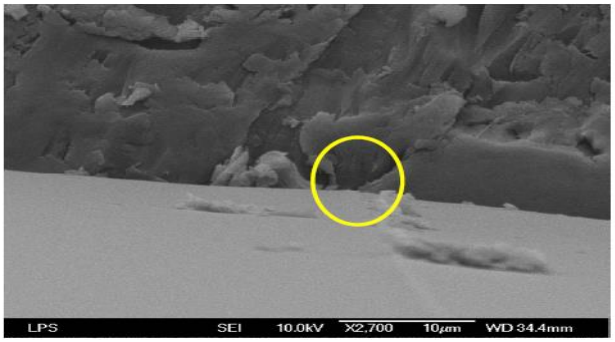

Collapsed microchannel after thermo-mechanical deformation at 70% strain

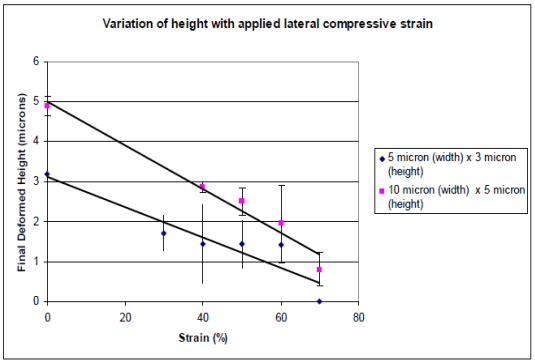

Comparison between reduction in heights for cases 2 and 3

It was observed that the reproducibility of the fabrication method worsened for higher deformation strains, as indicated by the increasing variance of the final deformed width measurements. This can be attributed to the variable viscous flow dynamics of the thermoplastic material during thermo-mechanical deformation. The uniformity in the flow of the material depends on the thermoplastic chip alignment accuracy with respect to the probes. Any misalignment, even minute, could have produced an amplified effect on the flow behavior at higher strains leading to inconsistent flow of the material. It was observed after thermo-mechanical deformation that in some of the deformed chips, the microchannel had collapsed whereas in some cases the deformation in microchannel was much less than expected. This anomalous behavior can be attributed to the inconsistent material flow dynamics as explained above along with manufacturing errors and assembly misalignments.

It can be inferred that in order to obtain a sub-micrometer wide channel from a rectangular initial microchannel, it is necessary to start with a low aspect ratio channel (width > height) with small initial dimensions. However, if the initial width of the microchannel is reduced to extremely small values, then the corresponding initial height should be further reduced. There is a limitation to doing this, as the enclosed microchannel is formed by thermal bonding procedure and shorter channels are prone to collapse during this process.

V. CONCLUSION

A novel fabrication process to develop a nanochannel from a microchannel with a rectangular cross-section, using thermo-mechanical deformation of thermoplastic chip containing that microchannel was evaluated in this thesis. The effects of shape and size of the initial microchannel on the deformation dynamics and final deformed microchannel dimensions were studied. A 2D, plane strain finite element model was developed in ANSYS® to estimate the deformation conditions required to deform microchannels with different shapes and sizes to sub-micrometer dimensions. A proof of concept was performed by mechanically deforming a PDMS microchannel to sub-micrometer dimensions.

Various thermo-mechanical deformation approaches were evaluated to heat the microchannel chip and then produce specific mechanical deformation in the heated chip. This lead to the design of a compact, custom mechanical rig to produce the thermo-mechanical deformation in the microchannel chip. The developed mechanical rig was optimized to produce the desired mechanical constriction effect on the microchannel. Microchannels with two different shapes and three different sizes in PMMA chips were thermo-mechanically deformed.

It was observed that the required compressive deformation strain and the final deformed channel dimensions depended on the aspect ratio (shape) and

the size of the microchannel. For higher aspect ratio microchannel, lower strains were required to reach sub-micrometer dimensions. However, the final deformed width of the microchannel varied considerably along its height and trans-micrometer openings were obtained along with a sub-micrometer width section across a cross-section of the deformed microchannel. The deformation was more sensitive to applied strain for high aspect ratio microchannels and thus precise control of deformed microchannel dimensions was impossible using the developed mechanical rig. As the aspect ratio was reduced, the strain required to deform the width of the microchannel to near micrometer dimensions increased. However, the required strain strongly depended on the size of the channel. For smaller microchannels with nearly the same aspect ratio, the strain required to reach near/sub micrometer widths was about 10% less than for bigger channels. Thus, it is recommended to deform a low aspect ratio microchannel with low initial crosssectional dimensions. But the size of the microchannel is limited by the lithography limitations and the thermal bonding process.

The consistency and efficiency of the fabrication process demonstrated was prone to manufacturing and assembly tolerances. The final deformed microchannel dimensions strongly depended upon and was extremely sensitive to the orientation of the chip in the mechanical rig, location and perpendicularity of the microchannel with respect to the deformation probes, width of the fixed boundary condition plates.

VI. FUTURE WORK

A ground-work for generation of nanochannel in polymer microfluidics chip was performed in this thesis. There are limitations to using a rectangular crosssection of the microchannel such as the variation in width of the deformed microchannel along its height and the dependence of the final deformed channel dimensions on the shape and size of the microchannel. Hence, different initial cross-sectional shapes of the microchannel should be explored which may eliminate problems faced in case of a rectangular microchannel as explained above. Some of the examples of microchannel cross-sectional shapes are rhombus or oval, which are broad at center and get narrower towards the top and bottom. It was observed that the reduction in width of the rectangular microchannel was maximum at its center under the action of applied, lateral compressive strain. Thus microchannels with rhombus or oval shaped cross-sections will deform is such a way that after thermo-mechanical deformation, there will not be any transmicrometer opening in the deformed microchannel cross-section. Thus, the requirement of fixed boundary conditions can be eliminated and the problems encountered due to bending in top and bottom side of the rectangular microchannels can also be eliminated.

This will also reduce the strain required to reach sub-micrometer dimensions. However, the fabrication of rhombus or oval shaped microchannels in thermoplastic fluidic chip is not trivial and considerable exploration will be needed in this field. The current mechanical deformation rig design can be modified to eliminate the out of plane bulk material flow and force all the material to flow towards the microchannel during the thermo-mechanical deformation process. Thus potential submicrometer wide channels can be obtained at lower, applied compressive strains. Following is a design based on this idea.

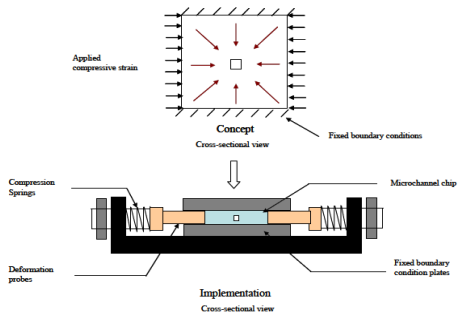

Modified mechanical rig design for higher deformation efficiency

In this modified rig design, the fixed boundary conditions completely cover the faces of the micro channel to prevent any material from bulging out of plane of the chip. Thus, all the material will be forced to move towards the channel under the action of applied compressive strain.

Another area of exploration is the deformation temperature. The deformation temperature can be reduced so as to increase the elastic modulus of the chip material. Thus, lower strains will be required to reduce the width of rectangular micro channel to sub-micrometer regime. However, it should be noted that large deformation force will be required to produce deformation in the chip. The model should be modified to account for the visco plastic behavior of the thermoplastic chip to better model the actual deformation conditions.

VII. REFERENCES

[1]. Alexe, M., C. Harnagea, Hesse, D. "Non-conventional micro- and nanopatterning techniques for electroceramics." Journal of Electroceramics, Vol. 12, No.1-2, Jan-Mar 2004, pp. 69-88

[2]. Becker, H. and C. Gartner. "Polymer microfabrication methods for microfluidic analytical applications." Electrophoresis, Vol.21, No.1, Jan 2000, pp. 12-26.

[3]. Bilenberg, B., S. Jacobsen, et al. "High resolution 100 kV electron beam lithography in SU-8." Microelectronic Engineering, Vol.83, No. 4-9, Apr-Sep 2006, pp. 1609-1612.

[4]. Chang, T. H. P. "Proximity effect in electron-beam lithography." Vacuum Science and Technology, Vol. 12 No.6, 1975, pp. 1271-1275.

[5]. Chapman, H. N., A. K. Ray-Chaudhari, et al. "First lithographic results from the extreme ultraviolet Engineering Test Stand." Vacuum Science and Technology, Vol. 19, No.6, 2001, pp. 2389-2395.

[6]. Chen, W. and H. Ahmed. "Fabrication of 5–7 nm wide etched lines in silicon using 100 keV electron-beam lithography and polymethylmethacrylate resist." Applied Physics, Vol.62, No.13, 2001, pp.1499-1501.

[7]. Chou, S. Y., P. R. Krauss, et al. "Nanoimprint lithography." Journal of Vacuum Science & Technology B (Microelectronics and Nanometer Structures), Vol.14, No.6, 1996

[8]. Guarini, K. W., C. T. Black, et al. "Nanoscale patterning using self-assembled polymers for semiconductor applications." Vacuum Science and Technology B, Vol.19, NO.6, October 2001, pp. 2784-2788.

[9]. Haneveld, J., H. Jansen, et al. "Wet anisotropic etching for fluidic 1D nanochannels." Journal of Micromechanics and Microengineering, Vol. 13, No.4, July 2003, pp. S62- S66.

[10]. Harnett, C. K., G. W. Coates, et al. "Heat-depolymerizable polycarbonates as electron beam patternable sacrificial layers for nanofluidics." Journal of Vacuum Science & Technology B (Microelectronics and Nanometer Structures), Vol.19, No.6, 2001.

[11]. Kameoka J., Jing N., et al Nanochannels for the identification of single molecules. SPIE Newsroom, The International Society of Optical Engineers, 2006.

[12]. Kaige, W., W. Pengye, et al. Fabricating nanofluidic channels and Applying it for single bio-molecule study. Engineering in Medicine and Biology 27th Annual Conference, Shanghai, China, Proceedings of the 2005 IEEE, 2005

[13]. Kim, E., Y. N. Xia, et al. "Micromolding in capillaries: Applications in materials science." Journal of the American Chemical Society, Vol.118, No.24, June 1996, pp. 5722-5731.

[14]. Kim, S. O., H. H. Solak, et al. "Epitaxial self-assembly of block copolymers on lithographically defined nanopatterned substrates." Nature, Vol.424, No. 6947, July 2003, pp. 411-414.

[15]. King, K. R., W. Chiaochun, et al. "Biodegradable polymer microfluidics for tissue engineering microvasculature." BioMEMS and Bionanotechnology. Symposium (Materials Research Society Proceedings, Vol.729, 2002.

[16]. Kovacs, G. T. A.Micromachined Transducers Sourcebook, WCB McGraw-Hill, 1998.

[17]. Kutchoukov, V. G., F. Laugere, et al. "Fabrication of nanofluidic devices using glass-to glass anodic bonding." Sensors and Actuators a-Physical, Vol. 114, No.2-3, Sept 2004, pp. 521-527.

[18]. Kutchoukov, V. G., L. Pakula, et al. "Fabrication of nanofluidic devices in glass with polysilicon electrodes." Sensors and Actuators a-Physica,l Vol.123-24, Sept 2005, pp. 602-607.

[19]. Mali, P., A. Sarkar, et al. "Facile fabrication of microfluidic systems using electron beam lithography." Lab on a Chip, Vol. 6, No.2, Feb 2006, pp.310-315.

[20]. Mao, P. and J. Han "Fabrication and characterization of 20 nm planar nanofluidic channels by glass–glass and glass–silicon bonding." Lab on a chip, Vol.5, June 2005, pp. 837-844.

[21]. Mijatovic, D., J. C. T. Eijkel, et al. "Technologies for nanofluidic systems: topdown vs. bottom-up—a review." Lab on a chip, Vol.5, No.5, 2005, pp.492-500.

[22]. Mullenborn, M., H. Dirac, et al. "Silicon Nanostructures Produced by Laser Direct Etching." Applied Physics Letters, Vol. 66 No. 22, May 1995, pp. 3001-3003.

[23]. Naulleau, P., K. A. Goldberg, et al. "Sub-70 nm extreme ultraviolet lithography at the Advanced Light Source static microfield exposure station using the engineering test stand set-2 optic." Journal of Vacuum Science & Technology B, Vol. 20 No. 6, Nov-Dec 2002, pp. 2829-2833.

[24]. Noerholm, M., H. Bruus, et al. "Polymer microfluidic chip for online monitoring of microarray hybridizations." Lab on a Chip , Vol. 4 No. 1 2004, pp. 28-37.

[25]. O'Brien II, M. J., P. Bisong, et al. "Fabrication of an integrated nanofluidic chip using interferometric lithography." Vacuum Science and Technology, Vol. 21 No. 6, 2003, pp. 2941-2945.

[26]. Park, M., C. Harrison, et al. "Block copolymer lithography: Periodic arrays of similar to 10(11) holes in 1 square centimeter." Science, Vol. 276, No. 5317, May 1997, pp. 1401-1404.

Cite this article as :

S. Lingamaiah , "Analysis of Deformation of Thermoplastics by Using Thermomechanical Process ", International Journal of Scientific Research in Science and Technology (IJSRST), Online ISSN : 2395-602X, Print ISSN : 2395-6011, Volume 10 Issue 1, pp. 86-112, January-February 2023. Available at doi : https://doi.org/10.32628/IJSRST21869
Journal URL : https://ijsrst.com/IJSRST21869